Kozumbo/NL

AD-A270 198

ION PAGE

Form Approved
OMB No. 0704-0188

1. AGENCY USE ONLY (Leave blank)

2. REPORT DATE: March 1993

3. REPORT TYPE AND DATES COVERED: Final, February 1992-January 1993

4. TITLE AND SUBTITLE
Numerical modelling of fringing fields and their use for complex permittivity measurements at high frequencies

5. FUNDING NUMBERS
AFOSR-91-0122
62202F
2312
AS

6. AUTHOR(S)
Camelia Gabriel

7. PERFORMING ORGANIZATION NAME(S) AND ADDRESS(ES)
King's College London
Strand
London WC2R 2LS

8. PERFORMING ORGANIZATION REPORT NUMBER

9. SPONSORING/MONITORING AGENCY NAME(S) AND ADDRESS(ES)
AFOSR/NL
110 Duncan Avenue, Suite B115
Bolling AFB DC 20332-0001
Dr Walter J. Kozumbo

10. SPONSORING/MONITORING AGENCY REPORT NUMBER

11. SUPPLEMENTARY NOTES

12a. DISTRIBUTION/AVAILABILITY STATEMENT
Approved for public release
distribution unlimited

93-23114

28pp

13. ABSTRACT (Maximum 200 words)

A technique was developed to measure the complex permittivity of materials using an open-ended coaxial probe in contact with a semi-infinite sample. It is based on a rigorous theoretical formulation of the admittance of the probe and was tested by measurements on standard solutions at frequencies of up to 20 GHz. The technique was further used to perform measurements on aqueous ionic solutions. The data were analysed and used to the develop models to predict the dielectric parameters of NaCl and KCl solutions at a given temperature as a function of concentration with the concentration range extending from pure water to saturated salt solutions.

The theoretical study and techniques were adapted to the measurement of thin samples in contact with the probe provided they are backed by a metallic plane. The success and range of applicability of the thin sample technique was tested with measurements on standard solutions.

Expressions were derived for the electric field in the medium terminating the probe. These expressions were used to determine the pattern of power deposition in the medium terminating the probe. Examples are given to illustrate this statement.

14. SUBJECT TERMS
Complex perrnittivity, ionic solutions, thin sample, power dissipation.

15. NUMBER OF PAGES
26

16. PRICE CODE

17. SECURITY CLASSIFICATION OF REPORT	18. SECURITY CLASSIFICATION OF THIS PAGE	19. SECURITY CLASSIFICATION OF ABSTRACT	20. LIMITATION OF ABSTRACT
(U)	(U)	(U)	(UL)

93 10 1 229

AFOSR-91-0122

NUMERICAL MODELLING OF FRINGING FIELDS AND THEIR USE FOR COMPLEX PERMITTIVITY MEASUREMENTS AT HIGH FREQUENCIES

Camelia Gabriel, PhD.

Physics Department
King's College London
London WC2R 2LS, UK.

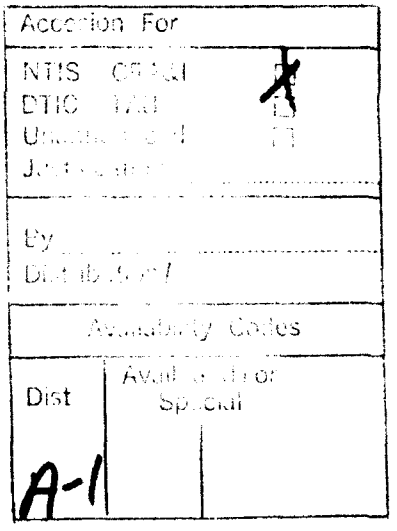

March 1993

Final Report for the Period 1 February 1992 - 31 January 1993

Prepared for

Armstrong Laboratory
Brooks Air Force Base TX 78235

TABLE OF CONTENTS

Figures

Tables

INTRODUCTION

The dielectric measurements of biological materials are increasingly being performed using network analysers and open-ended coaxial probes, a technique first introduced by Burdette *et al.* in 1980 [1]. Since then there has been an increasing interest in the use of open ended coaxial probes for dielectric measurements because of its suitability to a variety of applications in material science, chemical, biochemical and biomedical fields.

Measurements are made by placing the probe in contact with a sample and measuring its admittance or reflection coefficient using a network analyser or equivalent instrumentation. Theoretically, the most important consideration is the derivation of the relationship between the measured admittance or reflection coefficient and the dielectric properties of the sample. A number of simplifying assumptions are made during the course of the derivation which restricts the validity of the models to a certain range of parameters. We have examined the theoretical basis for the derivation of such models and their suitability for dielectric measurements on lossy materials in the frequency range 300kHz to 20 GHz.

Two situations were considered depending on the size of the sample in contact with the probe. First, it was assumed that the sample is homogeneous and occupies the entire half-space beyond the probe. The second case considered was that of a sample of finite thickness, placed between the probe and a conducting plane parallel to it.

The penetration of the electric field in the sample was determined and its dependence on the field frequency and the dielectric properties of the sample highlighted. The study of the field penetration is important because it helps delineate the extent of the sampling volume for a particular probe and frequency range. It is also important in its own right and may be used to assess the suitability of using an open-ended coaxial probes for applications other than dielectric measurements.

SEMI-INFINITE SAMPLE

Description Of The Problem

For the purpose of this analysis the coaxial probe is assumed to be axisymmetric, fitted with a ground plane that is large by comparison to its diameter and that in addition to the principal TEM mode only TM_{0n} evanescent modes that preserve cylindrical symmetry are generated at the interface. The problem is best described in the cylindrical coordinate system (ρ, ϕ, z) as illustrated in Figure 1 in which ε and μ are the absolute permittivity and permeability, the suffixes 0, 1 and 2 refer to air, the medium inside and outside the coaxial line respectively, ρ is the radial distance from the axis, ϕ the angular displacement around the axis and z the displacement along the axis. In the first instance we assume that the medium outside the probe is uniform and occupies the entire half-space beyond the ground plate.

Expression For The Electric And Magnetic Fields Inside The Line

The fields inside the line are a superposition of the forward travelling fundamental TEM mode, its reflection at the interface and the TM_{0n} evanescent modes generated at the discontinuity. The field components can be derived from electromagnetic theory in terms of the radial potential $\Phi(\rho)$ as

$$H_\varphi(\rho,z) = \frac{1}{\eta_1 \rho} a_0 \left[e^{-jk_1 z} - \Gamma e^{jk_1 z} \right] + \sum_{n=1}^{\infty} \left(\frac{-j\omega\varepsilon_1}{\gamma_n} \right) a_n e^{\gamma_n z} \frac{d\Phi_n(\rho)}{d\rho}, \quad (1)$$

$$E_\rho(\rho,z) = \frac{1}{\rho} a_0 \left[e^{-jk_1 z} + \Gamma e^{jk_1 z} \right] + \sum_{n=1}^{\infty} a_n e^{\gamma_n z} \frac{d\Phi_n(\rho)}{d\rho}, \quad (2)$$

$$E_z(\rho,z) = \sum_{n=1}^{\infty} \left(\frac{-p_n}{\gamma_n} \right) a_n e^{\gamma_n z} \Phi_n(\rho), \quad (3)$$

in which Γ *is the reflection coefficient of the TEM mode,* γ_n is the propagation constant of mode n

$$\gamma_n = \left[p_n^2 - k_1^2 \right]^{1/2} \quad (4)$$

and $k_1^2 = \omega^2 \mu_1 \varepsilon_1$ is the wave number, ω is the angular frequency and $\eta_1 = \sqrt{\mu_1 / \varepsilon_1}$ is the intrinsic impedance of the line. For n=0 (TEM mode) $p_0 = 0$, for $n > 0$ p_n is the nth root of

$$J_0(p_n b)\, Y_0(p_n a) - J_0(p_n a)\, Y_0(p_n b) = 0 \quad (5)$$

where J_0, Y_0 are the Bessel's functions of the first and second kinds of order zero, a and b the radii of the coaxial line.

For each n, the function Φ_n is obtained from

$$\Phi_n(\rho) = J_0(p_n\rho)\, Y_0(p_n a) - J_0(p_n a)\, Y_0(p_n\rho) \tag{6}$$

Finally, a_0 and a_n are amplitude terms normalised to the dimensions of the line and can be expressed in terms of the magnitude of the electric field at the aperture $E_\rho^a(\rho)$ at z=0 as

$$a_0 = \int_a^b E_\rho^a(\rho)d\rho \Big/ (1+\Gamma)\ln(b/a) \tag{7}$$

and

$$a_n = \int_a^b \Phi'(\rho)\rho E_\rho^a(\rho) \Big/ \int_a^b \Phi'^2(\rho)\rho d\rho \tag{8}$$

where and Φ' the derivative of Φ with respect to ρ.

Expression For The Electric And Magnetic Fields outside The Line

In dielectric medium 2 (z > 0) the magnetic field is expressed in terms of the electric field $E_\rho^a(\rho)$ at the aperture as

$$H_\varphi^+(\rho) = \frac{j\omega\varepsilon_2}{2\pi}\int_a^b\int_0^{2\pi} E_\rho^a(\rho')\cos(\varphi'-\varphi)\frac{e^{-jk_2R}}{R}\rho' d\varphi' d\rho' \tag{9}$$

In this derivation [2-4], the open end of the coaxial line is assumed to behave as a magnetic source radiating into the z > 0 region. The primed coordinates ρ' and φ' refer to a source point at the aperture while R the distance from the source to the corresponding field point which at z=0 is $R^2 = \rho^2 + \rho'^2 - 2\rho\rho'\cos(\varphi'-\varphi)$.

The aperture field $E_\rho^a(\rho)$ at z=0 can be obtained from (2) as

$$E_\rho^a(\rho) = \frac{1}{\rho}a_0(1+\Gamma) + \sum_{n=1}^{\infty} a_n \frac{d\Phi_n(\rho)}{d\rho} \tag{10}$$

Terminating Admittance For A Semi-Infinite Sample

The boundary conditions on the z = 0 plane require that the tangential electric and magnetic fields to be continuous. The continuity of the electric field is ensured by expressing the fields on either side in terms of E_ρ^a. From (1) and (9), the continuity of H_φ gives after substituting for a_0 and Γ

$$\frac{Y^a}{2\pi\rho}\int_a^b E_\rho^a(\rho)d\rho+\sum_{n=1}^{\infty}\left(\frac{-j\omega\varepsilon_1}{\gamma_n}\right)a_n\frac{d\Phi_n(\rho)}{d\rho}=\frac{j\omega\varepsilon_2}{2\pi}\int_a^b\int_0^{2\pi}E_\rho^*(\rho')\cos(\varphi'-\varphi)\frac{e^{-jk_2R}}{R}\rho'd\varphi'd\rho' \quad (11)$$

in which Y^a is the terminating admittance of a coaxial line given by $Y^a = Y_0(1-\Gamma/1+\Gamma)$ and $Y_0 = 2\pi/[\eta_1 \ln(b/a)]$. This expression was first derived and proposed for dielectric measurements by Mosig et al (1981) [5].

For n = 0, TEM propagation is assumed throughout, $E_\rho^a(\rho)$ is inversely proportional to ρ and expression (11) becomes

$$Y^a=\frac{j\omega\varepsilon_2}{[\ln(b/a)]^2}\int_a^b\int_a^b\int_0^{2\pi}\cos(\varphi'-\varphi)\frac{e^{-jk_2R}}{R}d\varphi'd\rho'd\rho \quad (12)$$

By expanding the exponential term in (2) into an infinite series and dropping the higher order terms in ω expression (2) becomes

$$Y^a = j\omega C\varepsilon_2 \quad (13)$$

in which C is a frequency independent constant whose value depends on the dimensions of the probe. By virtue of its derivation (13) is strictly valid at the limit of low frequencies. Expressions (11) and (12), derived in accordance with transmission line theory, should be expected to describe more adequately the aperture admittance of the probe.

Expressions (11), (12) and (13) are collectively described as models for the admittance of the probe in terms of the field frequency and the permittivity of the material in contact with it. However, only the simplest formulation (13) has an analytical solution, both (12) and (13) require numerical solutions.

NUMERICAL SOLUTIONS

Numerical solutions are approximate techniques that can reduce the rigour of the original derivation or impose numerical limits to its range of applicability. It is therefore important to report on the numerical implementation for models (12) and (13).

Method Of Moment Solution

The exact solution of (11) requires consideration of an infinite series of TM_{0n} modes and continuity of the fields over the entire a<ρ<b range. In practice, only a limited number of modes can be considered and matching can be explicitly satisfied at a limited number K of points between a and b [5,6]. Because of the axial symmetry this is equivalent to matching on K circles within the aperture. The interval [a,b] is thus divided into K subintervals with boundaries at ρκ with

the limits ρ_0= a and ρ_N = b. The potential in each ring is assumed constant with a value V_K such that $\rho E_\rho^a(\rho) = V_k$. Given that

$$\Gamma = -1 + \int_a^b E_\rho^a(\rho) d\rho / V \tag{14}$$

where V is the incident voltage amplitude. Expression (11) can be evaluated at the mid-point $\tilde{\rho}_l = (\rho_k + \rho_{k-1})/2$ of the every K interval from

$$\frac{2V}{\eta_1 \ln(b/a)} = V_k \sum_{k=1}^{k=K} \frac{\ln(\rho_k/\rho_{k-1})}{\eta_1 \ln(b/a)}$$
$$+V_k \tilde{\rho}_l \left(\frac{j\omega\varepsilon_1}{\gamma_n M_n^2} \sum_{k=1}^{k=K} \Phi_n'(\tilde{\rho}_l)\{\Phi_n(\rho_k) - \Phi_n(\rho_{k-1})\} + \sum_{k=1}^{k=K} \frac{j\omega\varepsilon_2}{2\pi} \int_a^b \int_0^{2\pi} \cos(\varphi' - \varphi) \frac{e^{-jk_2 R_1}}{R_1} d\varphi' d\rho' \right) \tag{15}$$

Equation (15) yields a set of K linear equations in V_k

$$\frac{2V}{\eta_1 \ln(b/a)} = \sum_{k=1}^{k=K} Y_{lk} V_k \tag{16}$$

that can be expressed in the matrix form

$$[I] = [Y_{lk}][V_k] \tag{17}$$

and solved in the usual way for V_k. The reflection coefficient can then be calculated from

$$\Gamma = -1 + \frac{1}{V} \sum_{k=1}^{k=K} V_k \ln(\rho_k/\rho_{k-1}) \tag{18}$$

In principle there is no restriction on the number of modes that are incorporated in the solution, in practice, including more than 10 modes makes almost no difference to the solution. The solution is more sensitive to the number of rings K. The solution corresponding to K=∞ is obtained by quadratic extrapolation [7] from solutions at 3 finite values of K.

Variational Solutions

There are three possible solutions for (12). First, the approach adopted by Misra (1987) [8] that consists in expanding the exponential term into a series and performing the triple integration on the individual terms. The expression for the admittance of the probe takes the form

$$Y^a = \omega C_0 \left(\varepsilon_2 C_1 + \varepsilon_2^2 \omega^2 C_3 + \varepsilon_2^{5/2} \omega^2 C_4 + \varepsilon_2^3 \omega^4 C_5 + \ldots . \varepsilon_2^{(N+1)/2} \omega^{N-1} C_N \right) \tag{19}$$

On evaluation the C_2 terms goes to zero. Misra considered only the first three terms, a solution that proved to be only marginally superior to the simple model (13). However this technique is computationally simple and more terms can easily be added without significant time penalty. By systematically adding

more terms we found that for frequencies in the GHz region and lossy materials the solution was sensitive to the number of terms N up to N=10.

An alternative solution of (12) would be to express the integral with respect to ϕ' in terms of Bessel functions, using an integral representation and the Neumann formula [4], which gives after changing the integration parameters

$$Y^a = Y_0 \frac{jk_2}{\ln(b/a)} \int_0^\infty \frac{1}{\xi(\xi^2 - k_2^2)^{1/2}} [J_0(\xi b) - J_0(\xi a)]^2 d\xi \tag{20}$$

where

$$(\xi^2 - k_2^2)^{1/2} = \begin{cases} 0, & \xi^2 > k_2^2 \\ \frac{\pi}{2}, & \xi^2 < k_2^2 \end{cases} \tag{21}$$

The integral is considered separately over the ranges $0<\xi<k_2$ and $k_2<\xi<\infty$. The integrand changes from imaginary to real at $\xi=k_2$, and the integration over these two ranges gives the aperture conductance G and susceptance B respectively. For $0<\xi<k_2$, the variable of integration is changed to $\xi=k_2\sin\theta$ while for $k_2<\xi<\infty$, the Dixon-Ferrar integral representation for the product of two Bessel functions is applied to transform the infinite integral into a finite integral of integral sines (Si). It follows that

$$Y^a = G + jB \tag{22}$$

where

$$G = \frac{Y_0}{\ln(b/a)} \frac{k_2}{k_1} \int_0^{\pi/2} \frac{d\theta}{\sin\theta} [J_0(k_2 a \sin\theta) - J_0(k_2 b \sin\theta)]^2 \tag{23}$$

$$B = \frac{Y_0}{\pi \ln(b/a)} \frac{k_2}{k_1} \int_0^{\pi/2} d\varphi \left\{ 2Si(k_2|u|) - Si\left(2ak_2 \left|\sin\frac{\varphi}{2}\right|\right) - Si\left(2bk_2 \left|\sin\frac{\varphi}{2}\right|\right) \right\} \tag{24}$$

where $u^2 = a^2 + b^2 - 2ab\cos\varphi$ and Si is the sine integral. These expressions are referred to as Macuvitz's formulation. Both (23) and (24) can be written as series expansions [9] that are convenient for numerical calculation.

The third and most straight forward solution for (12) is a direct evaluation after performing an integration transformation to convert the triple integral to a single integral that can be evaluated using Gaussian integration technique [10]. This is the technique we advocate. In principle, it is equivalent to the other techniques when the number of terms of their respective series expansion N tends to infinity. To illustrate this statement the three variational techniques were used to calculate the admittance of a Teflon filled probe of radial dimensions a = 0.456 mm, b = 1.490 mm, in contact with water, in the frequency

range 130 MHz to 20 GHz. The results showed that, for N=10, Marcuvitz's formulation agreed well with the direct solution; the exponential expansion solution (19) agreed with them for frequencies up to 7 GHz beyond which it became unstable.

FINITE THICKNESS SAMPLE

Expressions (11) and (12) can be adapted to the case of a dielectric sample of uniform but finite thickness backed by a conducting plane parallel to the ground plane of the probe. Both planes are assumed to be infinite in extent which is equivalent to neglecting the contribution to the reflection coefficient of the field behaviour at the bound. One way of performing this analysis is to use a technique known as the method of images. The aperture of the probe acts as a source of magnetic currents that gives rise to fields in the region of the dielectric sample and at the z = h plane. To maintain the boundary conditions at z = 0 and z = h require an infinite sequence of images of the source at z = 0 to be introduced at z = ± 2h, ± 4h.... In practice, only a limited number of images can be taken into consideration. For 2q images, expressions (11) and (12) become

$$\frac{1}{2\pi\rho}\int_a^b E_\rho^a(\rho)d\rho Y^a = \sum_{n=1}^{\infty}\frac{j\omega\varepsilon_1}{\gamma_n}\frac{d\Phi_n(\rho)}{d\rho}a_n + 2j\omega\varepsilon_2\int_a^b\int_0^{2\pi}E_\rho^a(\rho')\cos(\varphi'-\varphi)\Psi_q d\varphi' d\rho' \quad (25)$$

$$Y^a = \frac{4\pi\, j\,\omega\varepsilon_2}{[\ln(b/a)]^2}\int_a^b\int_a^b\int_0^{2\pi}\Psi_q\cos(\varphi'-\varphi)d\varphi' d\rho' d\rho \quad (26)$$

with

$$\Psi_q = \frac{e^{-jk_2R}}{4\pi R}\left\{1 + 2\sum_{q=1}\frac{R}{R_q}e^{\left[-jk_2(R_q-R)\right]}\right\} \quad (27)$$

and R_q is the distance from the source to a corresponding field point which at $z=2qh$ is $R_q^2 = R^2 + 4q^2h^2$.

Expressions (25) and (26) can be solved for the admittance of the probe using the numerical techniques detailed in the previous section. In the calculations reported here q = 30, the solution was not sensitive to further increase in the number of images.

FIELD PENETRATION AND ENERGY ABSORPTION IN THE SAMPLE

It is evident from the derivations of the previous sections that, except at the limit of low frequencies, the field in the z > 0 region is due to radiation from the principal TEM and higher order modes. The penetration of the field will depend on the frequency and the dielectric properties of the medium.

The field is derived from the assumption that the open end is equivalent to a source of magnetic current. The field distribution in the aperture plane takes

into account TEM and higher order modes. For a practical solution, the region between inner and outer conductors is subdivided into N concentric rings of boundaries ρ_{m-1} and ρ_m, there is a constant potential V_m within each ring. The field components can be expressed as

$$E_z = -\frac{1}{2\pi}\sum_{m=1}^{N} V_m \int_{\rho'=\rho_{m-1}}^{\rho_m}\int_{\phi'=0}^{2\pi} z(1+jk_2R)\cos\phi' \frac{e^{-jk_2R}}{R^3} d\phi' d\rho' \tag{28}$$

$$E_\rho = -\frac{1}{2\pi}\sum_{m=1}^{N} V_m \int_{\phi'=0}^{2\pi}\left[\frac{e^{-jk_2R}}{R}\right]_{\rho'=\rho_{m-1}}^{\rho_m} d\phi' \tag{29}$$

The power dissipated in the sample can then be calculated from

$$P = \sigma|E|^2 \tag{30}$$

where E is the resultant electric field and σ the total conductivity of the medium.

RESULTS

Semi-Infinite Sample

A study of all three admittance models given by expressions (11), (12) and (13) revealed the systematic difference between the predictions of (11) and (12) due to the contribution of higher order modes. It also showed, as expected, that the simple expression for the admittance (13) agrees with the other two models only at low frequencies and for low loss low permittivity materials. Model (13) was not considered further.

The predictions of models (11) and (12) were compared to corresponding experimental values of the admittance of the probe in contact with a number of standard liquids. The measurements were made using a network analyser calibrated using standard components prior to connecting the probe. Under these conditions the experimental values are expected to have scatter due to unwanted reflections from uncalibrated components. Typical sets of results are given in Figures 2 and 3. In Figure 2 the real and imaginary parts of the admittance of the probe in methanol are plotted as a function of frequency. In Figure 3 the results for water and formamide are given in the complex admittance plane. These results show that the experimental values do not agree closely with either model which leads to the conclusion that neither model is suitable for absolute measurements. However, relative measurements can be simply implemented by performing a calibration at the plane of the probe using the admittance model of choice to calculate the reflection coefficient of the standards used. This method has the added advantage of eliminating all unwanted reflections. Measurements using this technique and either of the two models produces accurate dielectric measurements in the frequency range up to 20 GHz as evident from Figure 4 which shows the dielectric spectrum of two standard liquids measured using (11)

and (12). An analysis of these data showed that the two set measurements are not significantly different from each other and from the previously published and accepted values.

Models (11) and (12) are therefore equally suitable for performing dielectric measurements at frequencies up to 20 GHz. The choice between them may therefore be made on the grounds of convenience since neither has been shown to be superior to the other. Model (11) requires a rather complex numerical solution for its implementation and, for this reason, is unsuitable for real time measurements. By contrast, model (12) can be solved directly using integral transformation and Gaussian integration techniques. To show the potential of the technique measurements were made on electrolyte solutions ranging in concentration from very dilute to the saturated solution. The results for KCl at 20°C are given in Table 1 as parameters of the Cole-Cole relationship

$$\varepsilon_s = \varepsilon_\infty + \frac{\varepsilon_s - \varepsilon_\infty}{1+(j\omega\tau)^{1-\alpha}} - \frac{j\sigma}{\omega\varepsilon_0} \tag{31}$$

in which σ is the ionic conductivity and all the parameters have their usual significance. The results for NaCl solutions are given in Table 2. The study of the variation of the parameters with concentration, which is not simply monotonic, carries information on the structure of the water in the solutions and on the presence and nature of water bound to the electrolyte. Examples of the concentration dependence of the dielectric parameters are as follows:

For NaCl at 25°C

$$\begin{aligned}
\varepsilon_s &= 78.3 - 1.86x + 2.84\times10^{-2}x^2 \\
\tau &= 8.1 + 7.26\times10^{-3}x - 1.04\times10^{-2}x^2 + 6.14\times10^{-4}x^3 \\
\sigma &= 1.61x - 2.64\times10^{-2}x^2 \\
\alpha &= 8.68\times10^{-3}x + 2.39\times10^{-4}x^2
\end{aligned} \tag{32}$$

For KCl at 20°C

$$\begin{aligned}
\varepsilon_s &= 80.1 - 1.60x + 4.18\times10^{-2}x^2 \\
\tau &= 9.3 - 5.69\times10^{-2}x - 6.84\times10^{-3}x^2 + 6.03\times10^{-4}x^3 \\
\sigma &= 1.72x - 1.46\times10^{-2}x^2 \\
\alpha &= 5.39\times10^{-3}x + 2.51\times10^{-4}x^2
\end{aligned} \tag{33}$$

where x is the concentration expressed as percentage by weight, the relaxation time is in picooseconds and the conductivity in siemens per metre. Previous data on the dielectric properties of ionic solution was available in a 1971 publication by Stogryn [10]. Stogryn's models were based on limited data and a Debye model was assumed without justification. The analysis of our data is still underway.

Finite Thickness Sample

Measurements performed using the finite thickness technique showed that for sample thicknesses h ≥ (b - a) results and conclusions similar to those obtained for the semi-infinite sample can then be reached. Both (25) and (26) have been used successfully to perform dielectric measurements and, provided that h ≥ (b - a), the accuracy of the measurements is not compromised by the choice of model. Table 3 gives the dielectric parameters of 4 standard liquids measured using this technique. The technique reverts to the case of a semi infinite sample when h tends to infinity. The dielectric parameters in Table 2 correspond to those of the general relationship

$$\varepsilon_s = \varepsilon_\infty + \frac{\varepsilon_s - \varepsilon_\infty}{\left[1 + (j\omega\tau)^{1-\alpha}\right]^\beta} - \frac{j\sigma}{\omega\varepsilon_0} \qquad (34)$$

which correspond to the Debye equation for $\alpha = 0$ and $\beta = 1$. It corresponds to the Cole-Cole equation for $\beta=1$ and $0<\alpha<1$ and to the Cole-Davidson relationship for $\alpha = 0$ and $0<\beta<1$.

Field Penetration And Power Dissipation

Calculations were made using (28), (29) and (30) for a Teflon filled probe of radial dimensions a = 0.456 mm, b = 1.490 mm for methanol, water and 0.9% NaCl solution (physiological saline) at three frequencies 200 MHz, 2.45 GHz and 20 GHz. The results are presented as follows:

Figure 5 a, b and c show the normalised power dissipation as a function of ρ, at z = 0.1mm, in the three samples, at the three frequencies respectively.

Figure 6 a, b and c show the normalised value of $|E|^2$ as a function of ρ, at z = 0.1mm, at the three frequencies, in the three samples respectively.

Figure 7 a, b, and c show the normalised value of $|E|^2$, as a function of ρ, for z values ranging from 0.1 to 3mm, at the three frequencies respectively.

These results show that in all cases, in the radial direction, the maximum power absorption occurs at the edge of the centre conductor. Beyond the centre conductor, the power dissipated decreases exponentially to a constant value as it approaches the radius of the outer conductor b, beyond which it suffers another exponential decay to vanishingly small values.

At a given distance (z=0.1mm) from the probe the power deposition depends on the dielectric properties of the sample. For example, at 200 MHz the highest power absorption occurs in NaCl due to its high conductivity. At 20 GHz the highest absorption occurs in methanol due to high field penetration.

From Figures 7 it can be seen that the bulk of power is absorbed in the terminating lossy media within the hemisphere subtended by the probe. Outside this volume the power absorbed in the samples is less than -25 dB at 200 MHz and 2.45 GHz but less than -20 dB at 20 GHz. This indicates that the ground plate is more important at the highest frequency.

CONCLUSIONS

The main purpose of this project was to develop an accurate technique to measure the complex permittivity of materials based on a rigorous theoretical formulation of the admittance of an open-ended coaxial probe. This has been achieved. The technique was tested by measurements on standard solution.

The new technique was used to perform a comprehensive study of ionic solutions. The extensive data obtained led to the development of models to predict the dielectric parameters of ionic solutions at a given temperature as a function of concentration.

The theoretical study and numerical techniques were extended to treat the case of a thin sample backed by a metallic plane. The technique was tested with standard solutions.

Further analysis led to the development of expressions for the field in the sample adjacent to the probe. This enabled the pattern of power deposition to be determined and improved our understanding of the sampled volume. More work is needed to determine the power deposition in biological material.

REFERENCES

1. Burdette E.C., F.L. Cain and J. Seals. In vivo probe measurement technique for determining dielectric properties at VHF through microwave frequencies. IEEE Trans. Microwave Theory Tech., Vol. MTT-28:.414-427, 1980.

2. Levine H.R. and C.H. Papas. Theory of circular diffraction antenna. J. Appl. Phys., Vol.22:.29-43, 1951.

3 Marcuvitz N. Wavelength Handbook. New York: McGraw-Hill, 1951.

4. Galejs J. Antennas in Homogeneous Media. Oxford, England: Pergamon, 1969.

5. Mosig J.R., J.C.E. Besson, M. Gex-Fabry and F.E. Gardiol. Reflection of an open-ended coaxial line and approximation to non-destructive measurement of materials. IEEE Trans. Instrum. Meas., Vol.IM-30: 46-51, 1981.

6. Nevels,R.D., C.M. Butler and W. Yablon. The annular slot antenna in a lossy biological medium. IEEE Trans. Microwave Theory Tech., Vol.MTT-33: 314-319, 1985.

7. Jenkins S., A.W.Preece, T.E. Hodgetts, G.T. Symm, A.G.P. Warham, R.N. Clarke. Comparison of three numerical treatments for the open-ended coaxial line sensor. Electronics Letters, Vol.26: 234-236, 1990.

8. Misra,D.K. A quasi-static analysis of open-ended coaxial lines. IEEE Trans. Microwave Theory Tech., Vol.MTT-35: 925-928, 1987

9. Misra D.K., M. Chabbra, B.R. Epstein, M. Mirotznik and K.R. Foster. Noninvasive electrical characterization of materials at microwave frequencies using an open-ended coaxial line. IEEE Trans. Microwave Theory Tech., Vol. 38(1): 8-14, 1990.

10 Warham, A.G.P. Annular slot antenna radiation into lossy material", NPL (UK) Report DITC 152/89, 1989.

11 Stogryn, A. Equations for calculating the dielectric constant of saline water. IEEE Trans. Microwave Theory Tech., MTT-19: 733-735, 1971.

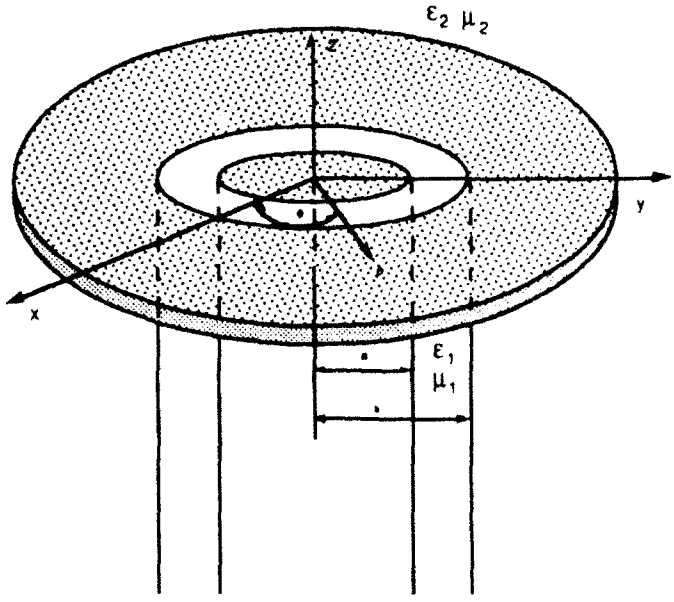

Figure 1. A probe of inner and outer radii a and b respectively.

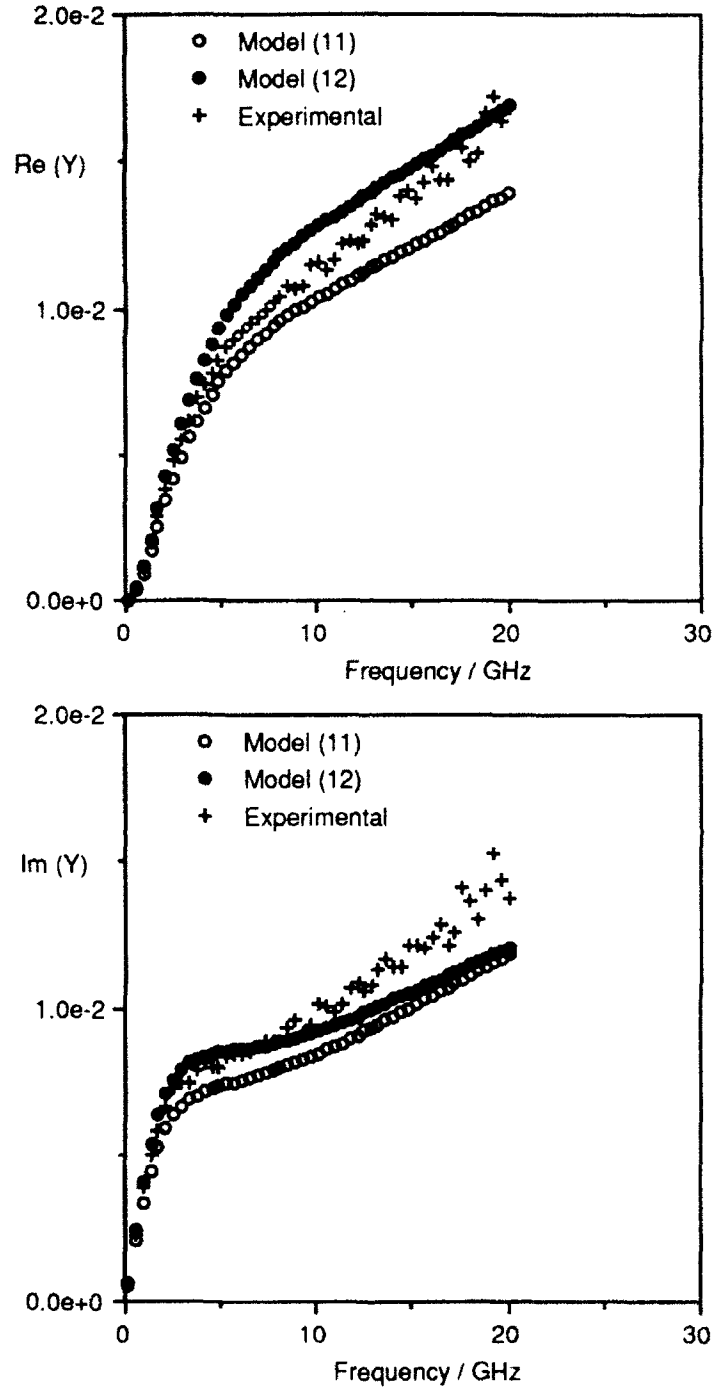

Figure 2. Admittance of probe in methanol at 20°C: (a) Real , (b) Imaginary part.

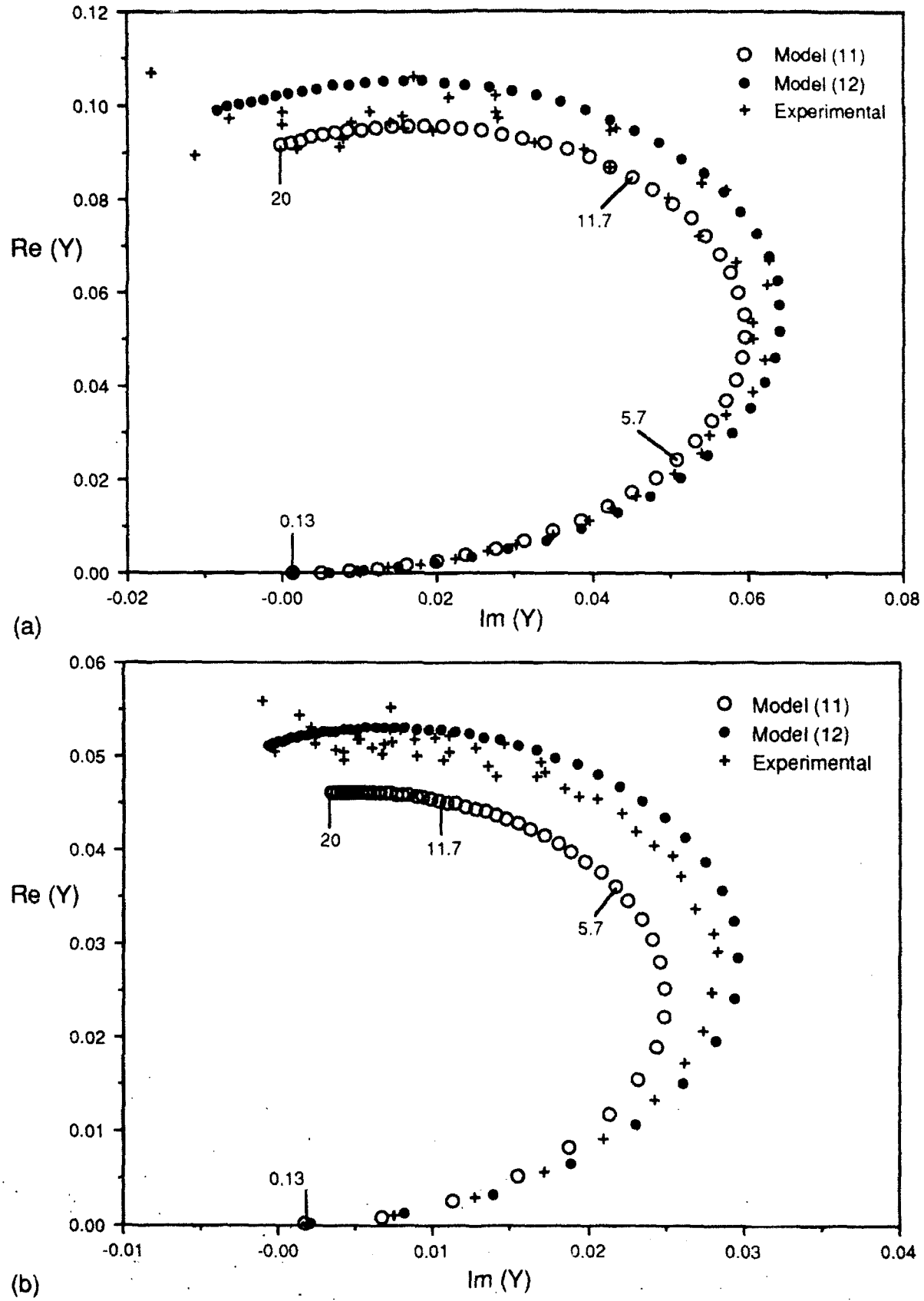

Figure 3. Complex admittance of probe in (a) water, (b) formamide. (The numbers are frequencies in GHz).

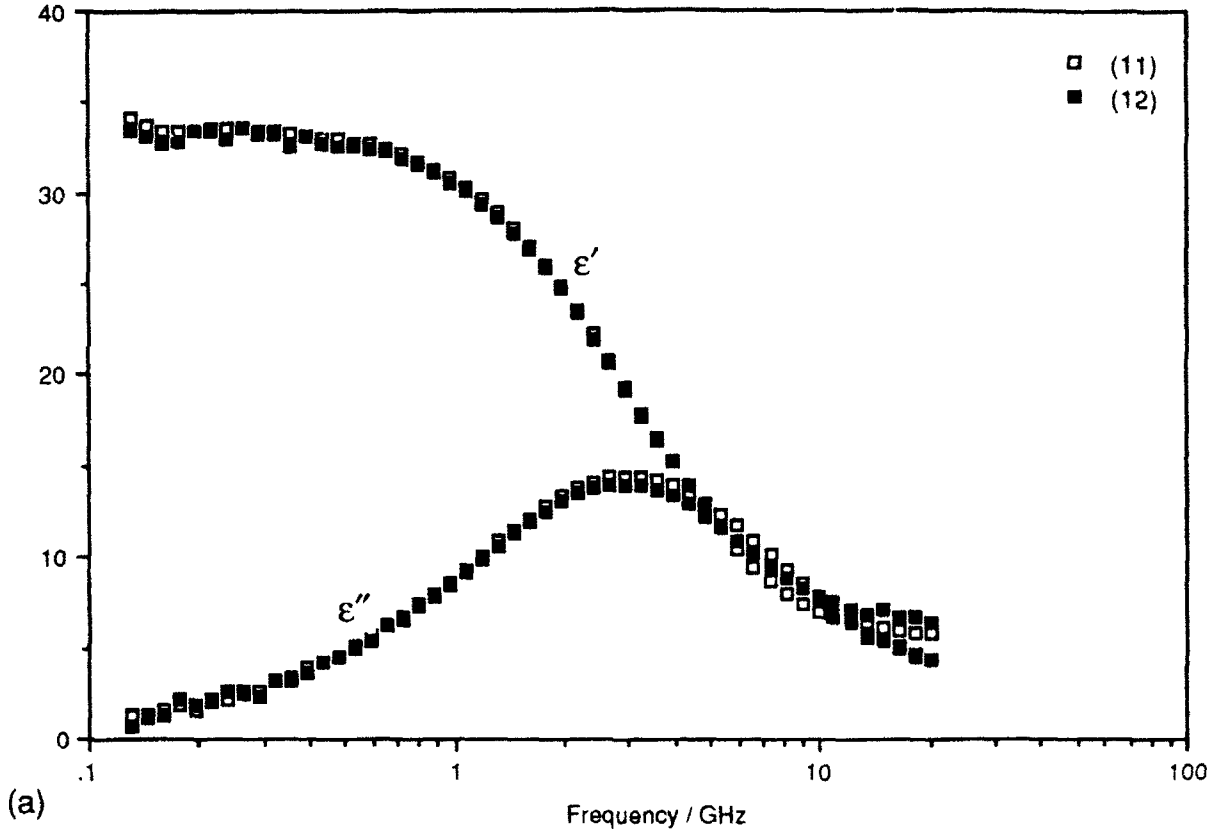

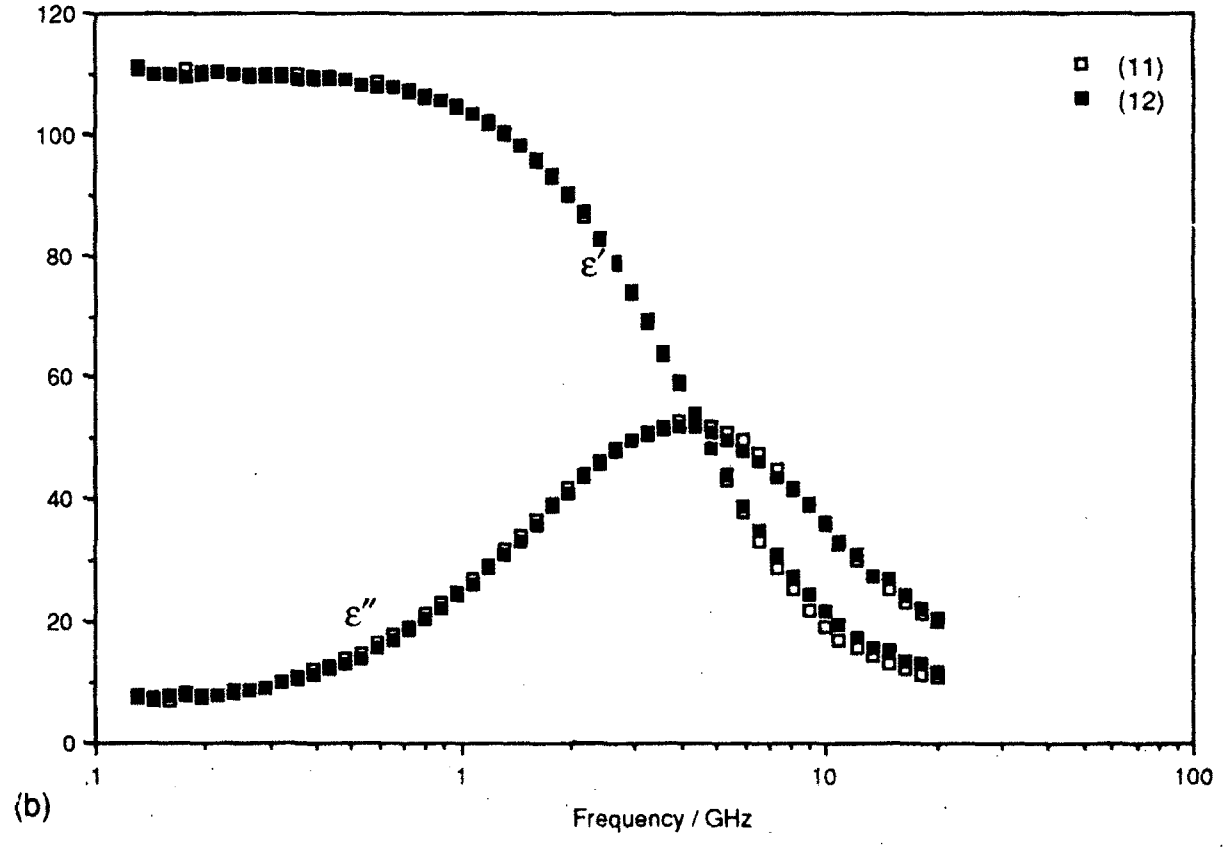

Figure 4. Dielectric Properties of standard liquids (a) Methanol, (b) Formamide at 20°C.

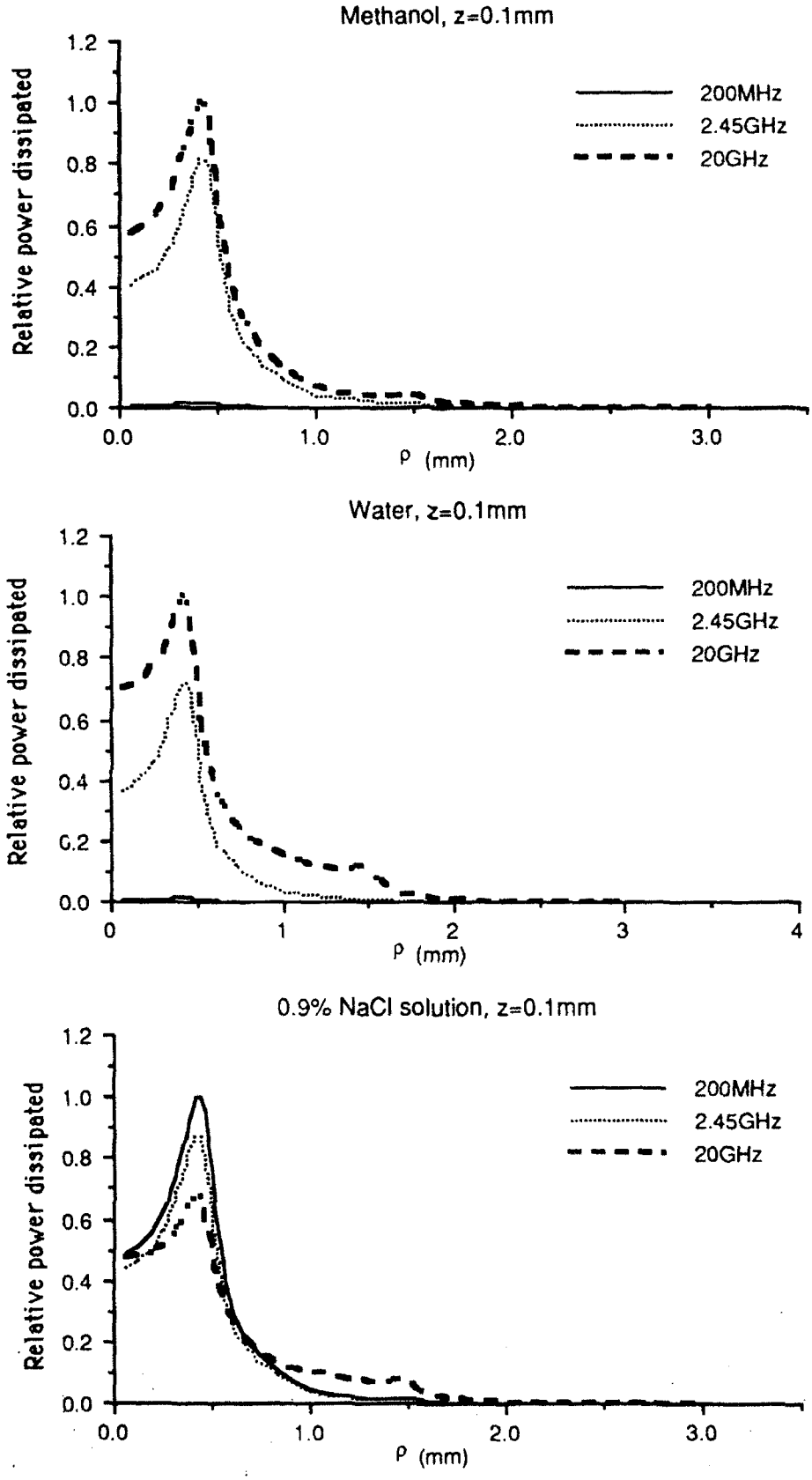

Figure 5. Relative power dissipated from the probe in 3 samples at 3 different frequencies.

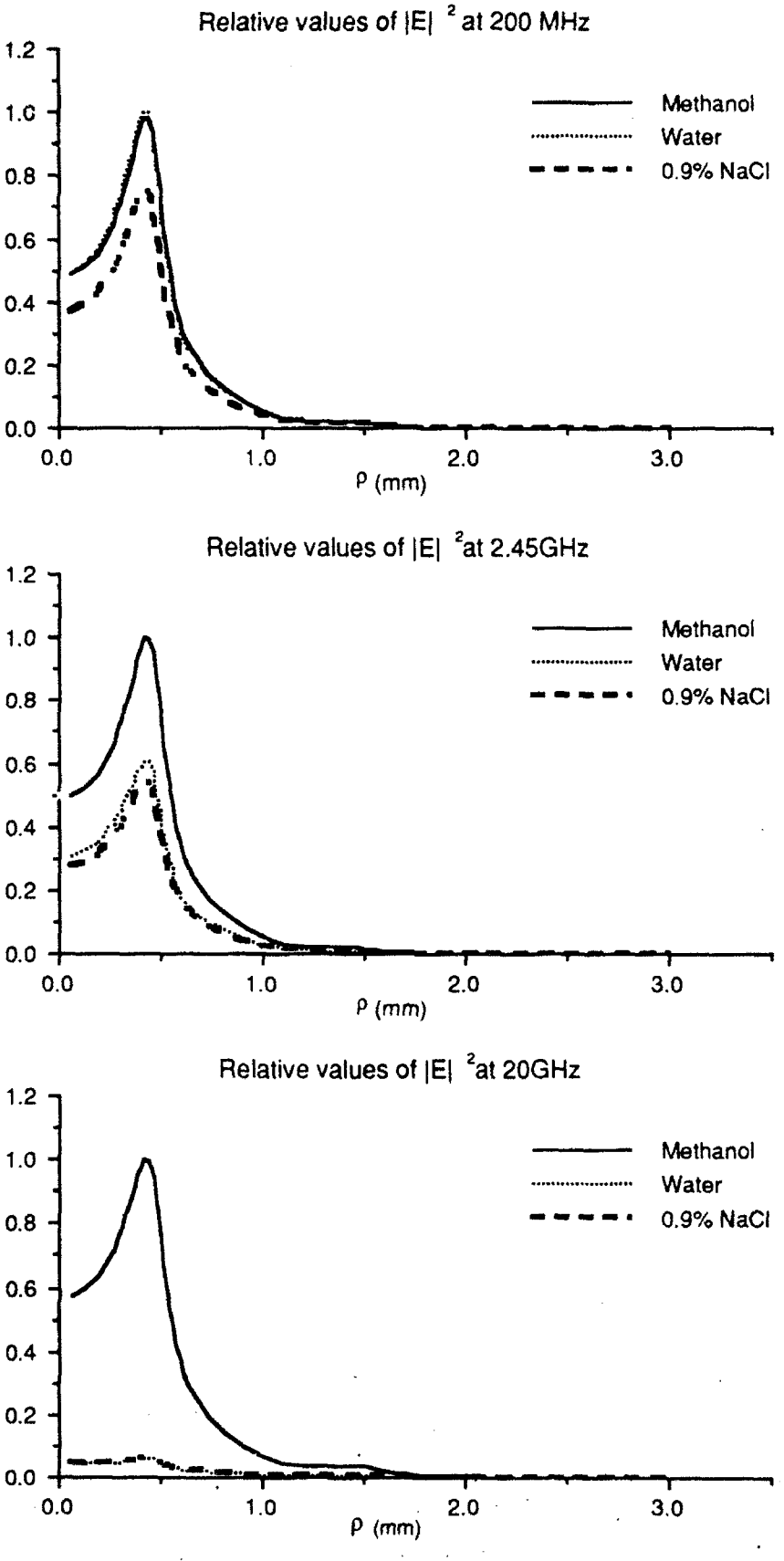

Figure 6. Relative value of the square of the electric field at 3 different frequencies, in 3 samples.

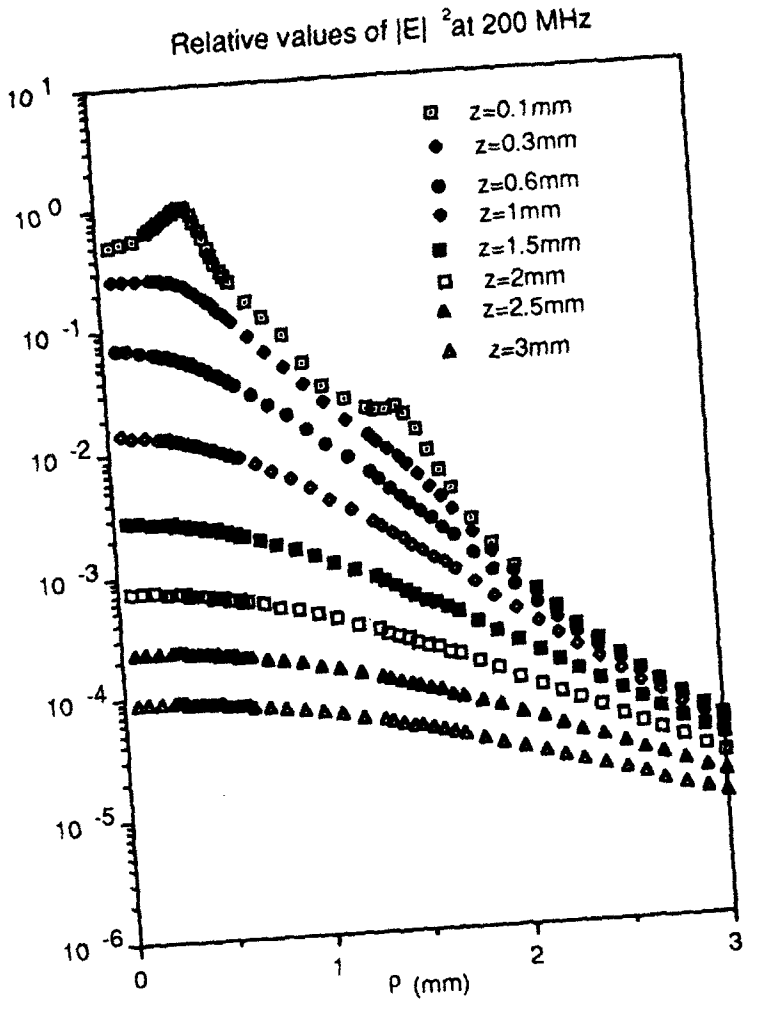
Relative values of |E| ²at 200 MHz
10 1
10 0
10 -1
10 -2
10 -3
10 -4
10 -5
10 -6
0
1
2
3
ρ (mm)
z=0.1mm
z=0.3mm
z=0.6mm
z=1mm
z=1.5mm
z=2mm
z=2.5mm
z=3mm

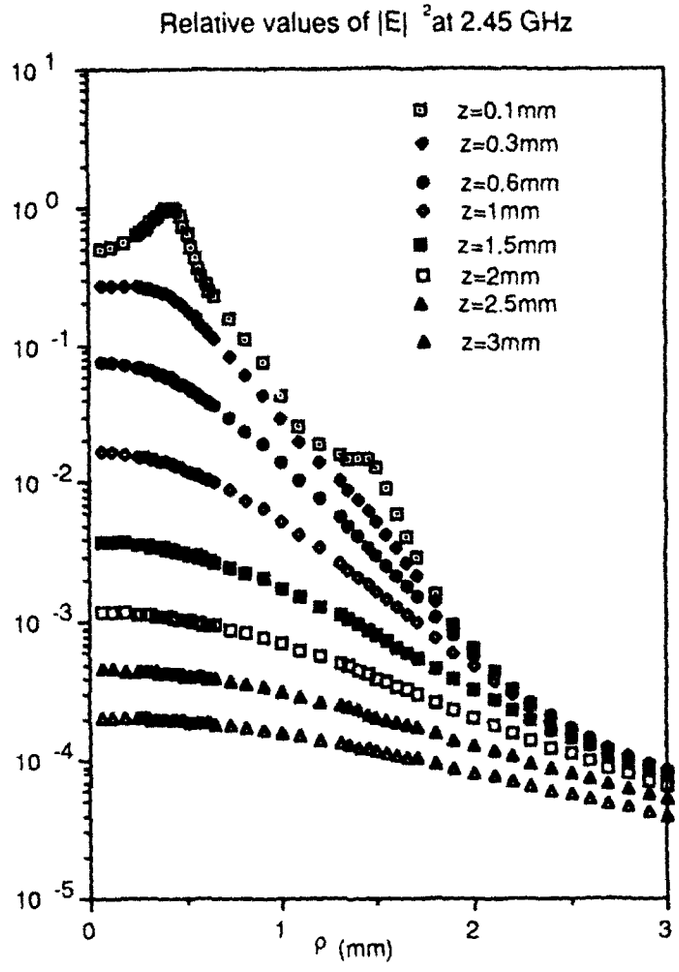
Relative values of |E| ²at 2.45 GHz
10 1
10 0
10 -1
10 -2
10 -3
10 -4
10 -5
0
1
2
3
ρ (mm)
z=0.1mm
z=0.3mm
z=0.6mm
z=1mm
z=1.5mm
z=2mm
z=2.5mm
z=3mm

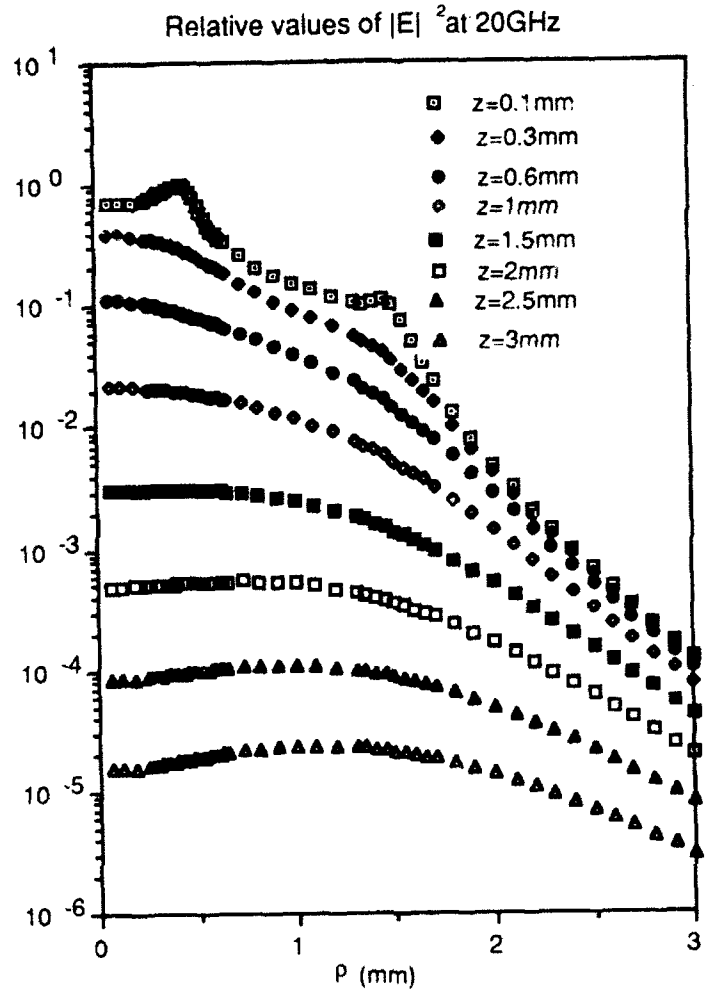

Figure 7. Relative value of the square of the electric field, in water, at 3 different frequencies.

TABLE 1. Dielectric parameters of KCl solutions obtained by analysis of the experimental results at 20°C. The Δ terms correspond to the 95% confidence interval.

Conc. %	ε_S	$\Delta\varepsilon_S$	τ (ps)	$\Delta\tau$ (ps)	α	$\Delta\alpha$	σ (Sm^{-1})	$\Delta\sigma$ (Sm^{-1})
25.6	66.83	1.45	13.50	0.78	0.306	0.020	34.528	0.067
20.5	64.48	0.27	10.30	0.11	0.218	0.006	29.271	0.015
15.3	65.34	0.33	8.89	0.13	0.142	0.010	22.967	0.017
12.8	66.21	0.25	8.80	0.10	0.096	0.008	19.576	0.011
10.2	68.09	0.20	8.75	0.08	0.071	0.007	16.021	0.009
7.67	70.53	0.16	8.77	0.06	0.054	0.005	12.250	0.007
5.12	73.30	0.23	8.83	0.09	0.045	0.007	8.447	0.008
2.56	76.44	0.11	8.99	0.04	0.031	0.003	4.456	0.004
2.05	77.08	0.09	9.09	0.03	0.017	0.003	3.552	0.003
1.53	77.81	0.08	9.16	0.03	0.014	0.002	2.712	0.003
1.28	78.13	0.04	9.06	0.02	0.023	0.001	2.334	0.001
1.02	78.67	0.13	9.18	0.05	0.016	0.004	1.849	0.003
0.767	79.15	0.12	9.19	0.05	0.021	0.004	1.418	0.002
0.512	79.43	0.08	9.20	0.04	0.012	0.003	0.959	0.001
0.256	79.81	0.08	9.21	0.04	0.012	0.003	0.500	0.002
0.205	80.00	0.07	9.29	0.03	0.009	0.002	0.404	0.001
0.153	80.01	0.06	9.26	0.03	0.011	0.002	0.307	0.001
0.128	79.94	0.06	9.19	0.02	0.013	0.002	0.258	0.001
0.102	80.09	0.07	9.26	0.03	0.012	0.002	0.208	0.001
0.0767	79.91	0.05	9.15	0.02	0.011	0.001	0.159	0.001
0.0512	80.02	0.06	9.21	0.02	0.008	0.002	0.107	0.001
0.0256	80.01	0.05	9.17	0.02	0.009	0.001	0.054	0.001

TABLE 2. Dielectric parameters of NaCl solutions obtained by analysis of the experimental results at 25°C. The Δ terms correspond to the 95% confidence interval.

Conc. %	ε_S	$\Delta\varepsilon_S$	τ (ps)	$\Delta\tau$ (ps)	α	$\Delta\alpha$	σ (Sm^{-1})	$\Delta\sigma$ (Sm^{-1})
24.65	49.63	1.37	11.20	0.93	0.354	0.028	23.521	0.053
20.6	52.51	0.93	9.10	0.44	0.287	0.023	21.976	0.046
10.89	61.21	0.27	7.79	0.10	0.112	0.009	14.277	0.016
5.64	68.52	0.15	7.92	0.05	0.048	0.005	8.166	0.009
3.77	72.08	0.21	8.00	0.09	0.052	0.007	5.701	0.007
1.91	74.90	0.13	8.05	0.05	0.021	0.004	3.085	0.004
0.73	77.07	0.12	8.04	0.05	0.017	0.004	1.266	0.002

TABLE 3. Dielectric parameters of standard liquids obtained by analysis of the experimental results on finite thickness samples at 20°C. The Δ terms correspond to the 95% confidence interval.

h(mm)	ε_S	$\Delta\varepsilon_S$	ε_∞	$\Delta\varepsilon_\infty$	τ(ps)	$\Delta\tau$ (ps)	$\sigma(Sm^{-1})$	$\Delta\sigma(Sm^{-1})$	β	$\Delta\beta$
Methanol										
1.0	33.8	0.2	5.0	0.3	50.2	1.1	-	-	-	-
1.5	35.3	0.2	4.6	0.2	54.0	0.7	-	-	-	-
2.0	34.6	0.1	4.4	0.1	53.3	0.4	-	-	-	-
3 0	34.7	0.1	4.6	0.1	54.0	0.3	-	-	-	-
∞	33.7	0.03	4.85	0.04	53.8	0.2	-	-	-	-
Ethanol										
1.0	25.3	0.3	4.6	0.2	173	5	-	-	-	-
1.5	27.2	0.2	4.4	0.2	164	4	-	-	-	-
2.0	25.7	0.2	4.2	0.1	174	3	-	-	-	-
3.0	26.2	0.2	4.2	0.1	176	3	-	-	-	-
∞	25.1	0.1	4.22	0.08	179	2	-	-	-	-
Ethanediol										
1.0	42.4	0.2	3.1	0.3	170	5	-	-	0.73	0.02
1.5	43.3	0.2	3.0	0.3	162	5	-	-	0.75	0.02
2.0	42.3	0.1	3.4	0.2	156	3	-	-	0.77	0.02
3.0	42.6	0.1	3.6	0.2	158	3	-	-	0.82	0.01
∞	42.0	0.01	3.66	0.02	162	0.3	-	-	0.806	0.001
Formamide										
1.0	110.3	0.4	5.2	0.7	36.8	0.5	0.037	0.007	-	-
1.5	112.1	0.5	5.3	0.8	38.1	0.6	0.038	0.008	-	-
2.0	110.8	0.3	5.5	0.4	36.9	0.3	0.035	0.004	-	-
3.0	111.4	0.2	5.1	0.3	37.7	0.2	0.031	0.003	-	-
∞	111	0.06	5.7	0.1	40.0	0.08	0.028	0.001	-	-